ISSN 1063-7834, Physics of the Solid State, 2019, Vol. 61, No. 2, pp. 214–224. © Pleiades Publishing, Ltd., 2019.
Russian Text © I.K. Razumov, Yu.N. Gornostyrev, A.E. Ermakov, 2019, published in Fizika Tverdogo Tela, 2019, Vol. 61, No. 2, pp. 346–356.

PHASE TRANSITIONS

Nonequilibrium Diffusional Phase Transformations in Alloys Induced by Migration of Grain Boundaries and Dislocations

I. K. Razumov[a, *], Yu. N. Gornostyrev[a, b], and A. E. Ermakov[a, b]

[a] *Mikheev Institute of Metal Physics, Ural Branch, Russian Academy of Sciences, Yekaterinburg, 620108 Russia*

[b] *Ural Federal University Named after the First President of Russia B.N. Yeltsin, Yekaterinburg, 620002 Russia*

**e-mail: rik@imp.uran.ru*

Received September 25, 2018

Abstract—The main scenarios of nonequilibrium diffusional transformations induced by moving defects (dislocations, grain boundaries) in alloys under severe plastic deformation are considered. It has been shown that the phase state locally changes in the area of a defect where thermodynamic properties of alloy are locally changed, and the attained state is frozen after the displacement of a defect due to the difference between the rates of bulk diffusion and diffusion on a defect. For this reason, an alloy shifts from the state of its thermodynamic equilibrium under treatment, thus different nonequilibrium states, such as the disordering of alloy, the dissolution of equilibrium phase precipitates, the appearance of nonequilibrium phases, and the formation of regular structures, are possible depending on the type of the system. These effects may take place if the treatment of an alloy is performed at moderate temperatures, when diffusion is frozen in the bulk and rather active on defects. The phenomena of phase and structural instability developing under severe plastic deformation at moderate temperatures are considered within the framework of the proposed model.

DOI: 10.1134/S1063783419020215

1. INTRODUCTION

In recent decades, great attention is attracted by the unordinary phase and structural transformations occurring in alloys under severe plastic deformation (SPD) or further thermal treatment. In particular, among them are the disordering and amorphization of alloys [1, 2], the formation of supersaturated solid solutions of immiscible components [3, 4], the decomposition with the precipitation of nonequilibrium phases [5, 6], the cyclic reactions [7], the formation of modulated structures (patterns) stable under continued treatment [8, 9], and the abnormally fast appearance of low-temperature phases [10, 11] and broad grain boundary segregations [12–14].

In principle, the disordering and abnormal mechanical alloying processes can be understood in terms of immediate mixing of atoms due to the development of sliding bands in mutually intersecting planes [15–17]. On the other hand, the observed acceleration of abnormal mechanical alloying during the transition to a nanocrystalline state [18, 19], when the penetration of dislocations into the volume of a grain is complicated [20], cannot be understood by the mechanism proposed in [15–17]. It seems undoubtful that diffusion mass transfer processes must also be taken into account at moderate temperatures alongside with mixing processes. In particular, the phenomena of the decomposition and appearance of low-temperature phases under SPD at room temperature argue for the occurrence of abnormally fast diffusion. Estimates show that the transformations implemented in this case are probably due to the diffusion over dislocations and grain boundaries with the participation of nonequilibrium point defects [10, 13, 21, 22] generated under SPD conditions.

Diffusion on dislocations and grain boundaries (GBs) not only provides the accelerated development of equilibrium phase transformations, but also leads to the realization of nonequilibrium phase and structural states. In particular, the effect of the "diffusion cutting" of precipitates by dislocations is well known [23–25] and considered one of the main reasons for the dissolution of intermetallide particles and carbide precipitates in steels under SPD [4]. It is noteworthy that the authors [23–25] take into account only the elastic interaction between atoms and dislocations. However, it is currently uncontroversial that the elastic contribution is hardly the only one determining the interaction between dissolved atoms and other lattice defects [26]. A more essential part may be played by the change in the energies of chemical bonds upon the displacement of atoms from the volume of a precipitate into the area of a defect (see, e.g., [26, 27]), and this is also must be

taken into account when constructing a sequential model.

The "diffusion cutting" model [23–25] considers the evolution of the shape of a precipitate in a field of stresses created by an ensemble of edge dislocations at the phase interface. Meanwhile, the driving force of the migration of defects is rather great under SPD conditions and may lead to the mechanical cutting of (semi)coherent precipitates by dislocations [28, 29]. The multiple cutting of precipitates by dislocations leads to their reduction in size and the mixing of atoms [15–17]. In this case, bulk diffusion does not always act as a competing factor and may even promote the dissolution of precipitates in certain cases [30]. However, the models [15–17] do not take into account the diffusion processes developing on dislocations at moderate temperatures. It has been shown in the work [31] that the change in the thermodynamic properties of an alloy (segregation, mixing, and ordering energy) in the cores of dislocations cutting a precipitate may stimulate the local development of a nonequilibrium transformation. The attained state is frozen upon the displacement of a dislocation, and the state of an alloy shifts from its thermodynamic equilibrium during treatment.

The effect of the dissolution of precipitates by moving grain boundaries was revealed for the first time in the work [32] and is usually observed at increased temperatures under recrystallization conditions [33–35]. It may be expected that similar processes also develop in the case of SPD under low-temperature dynamic recrystallization [36]. Based on the calculation results [37, 38] for the impurity concentration profile near a moving GB, it has been shown in work [35] that small precipitates are dissolved in the depleted zone near a grain boundary, if their size is comparable with the width of this zone, and the GB motion velocity is not very high. There are no models considering the motion of a grain boundary through a precipitate in the literature. Meanwhile, it is possible to expect that this process will lead to an appreciable change in the phase state of an alloy under SPD when the driving force of the migration of grain boundaries is rather high.

When analyzing the phase transformations induced by the migration of grain boundaries, it is necessary first of all to consider the segregations on moving GBs, as done in works [37–42]. In papers [37, 38], attention was focused on a steady-state regime to conclude that segregation is less pronounced at the moving GB in comparison with a motionless one. However, the segregation formation stage is important at moderate temperatures in dilute alloys, while no steady states can be attained for any reasonable time periods. In works [41, 42], the segregation formation kinetics was modeled to demonstrate, in particular, that the impurity concentration attained on a grain boundary in certain special regimes of motion can be higher than in a steady-state regime.

Hence, it may be expected that moving dislocations and grain boundaries can have an appreciable effect on the development of phase transformations under SPD. In this work, we demonstrate that the diffusion on the migrating GBs and dislocations at moderate temperatures may lead to a great variety of nonequilibrium phase transformations including fast disordering, the appearance of nonequilibrium phases, and the formation of supersaturated solid solutions and dissipative structures. When defects migrate, mechanical energy is converted into the internal energy of an alloy, which shifts from the state of its thermodynamic equilibrium.

2. MODEL FORMULATION

In the mean field approximation, the free energy density for ordered AB alloy can be written in the form [43–45]

$$f(c,\mathbf{r}) = \varepsilon(\mathbf{r})c + \nu(\mathbf{r})c^2 + \theta(\mathbf{r})\eta^2 + \frac{kT}{2}\sum_n [c^{(n)}\ln c^{(n)} + (1-c^{(n)})\ln(1-c^{(n)})], \quad (1)$$

where $\varepsilon(\mathbf{r})$, $\nu(\mathbf{r})$, and $\theta(\mathbf{r})$ are the dissolution, mixing, and ordering energies, and $c = (c^{(1)} + c^{(2)})/2$ and $\eta = (c^{(1)} - c^{(2)})/2$ are the local concentration of a selected component and the local degree of ordering, which are related with the sublattice concentrations, with summation over two sublattices ($n = 1, 2$). Let us note that Eq. (1) for the free energy is valid for the alloys, whose ordering can be described by the one family of concentration waves (one ordering parameter) [43].

We consider a structurally nonuniform alloy, assuming that the parameters $\varepsilon(\mathbf{r})$, $\nu(\mathbf{r})$, and $\theta(\mathbf{r})$ may depend on the coordinates; in particular, they are locally changed in the region of structural defects (dislocations and grain boundaries). In the absence of decomposition or ordering, the nonuniformity in the distribution of component B is due to dissolution energy change

$$\varepsilon(\mathbf{r}) = \varepsilon_b + \delta\varepsilon\Omega(\mathbf{r} - \mathbf{r}_{\text{def}}), \quad (2)$$

where $\delta\varepsilon = \varepsilon_{\text{def}} - \varepsilon_b$ is the energy of the impurity segregation on a defect, and $\Omega(\mathbf{r} - \mathbf{r}_{\text{def}})$ is the disturbance shape function near a defect, differs from zero in a narrow area with a width d, and quickly descends down to zero with increasing distance (see Appendix). The mixing and ordering energy changes in the area of a defect can be determined in the same fashion:

$$\nu(\mathbf{r}) = \nu_b + \delta\nu\Omega(\mathbf{r} - \mathbf{r}_{\text{def}}),$$
$$\theta(\mathbf{r}) = \theta_b + \delta\theta\Omega(\mathbf{r} - \mathbf{r}_{\text{def}}). \quad (3)$$

Hence, a structural defect is modeled in the form of a narrow area, within which the properties of an alloy differ from the bulk ones. We assume that a defect

moves at a velocity V_{def} such that its position is given by the radius vector

$$\mathbf{r}_{GB}(t) = \mathbf{r}_{GB}^{(0)} - \mathbf{V}_{def}t.$$

In such an approach, dislocations and grain boundaries differ from each other only by the dimension of a defect and the parameters describing its interaction with impurity atoms. This provides the possibility to consider the interaction of dislocations and grain boundaries with precipitates within the same approach.

The evolution in the distribution of alloy components with time is determined by the continuity equation [44, 46]

$$\frac{dc}{dt} = -\nabla J, \quad J = -\frac{D(\mathbf{r})c(1-c)}{kT}\nabla\left(\frac{\delta F}{\delta c}\right), \tag{4}$$

where $F(c)$ is the Ginzburg–Landau functional

$$f = \int\left[f(c,\mathbf{r}) + \frac{\sigma R^2}{2}[(\nabla c)^2 + (\nabla\eta)^2]\right]d\mathbf{r}. \tag{5}$$

Here, σ is the surface energy of precipitates, and R is the parameter characterizing the phase interface width. The diffusion coefficient $D(r)$ must take into account the difference between the rates of diffusion in the volume and on a defect, i.e.,

$$D(\mathbf{r}) = D_b + (D_{def} - D_b)\Omega(\mathbf{r} - \mathbf{r}_{def}). \tag{6}$$

Finally, let us describe the evolution of the order parameter η using the Allen–Cahn relaxation equation [47]

$$\frac{d\eta}{dt} = -M(\mathbf{r})\frac{\delta F}{\delta\eta}, \tag{7}$$

where $M(\mathbf{r}) = \kappa_0 D(\mathbf{r})/kT$ is the coefficient characterizing the frequency of atom jumps between different sublattices, $\kappa_0 \sim a^{-2}$, and a is the lattice constant [31, 44]. Let us note that the used approach implies a smooth change in the order parameters $c(\mathbf{r})$, $\eta(\mathbf{r})$ depending on the coordinate, and this is a certain approximation sufficient to demonstrate the qualitative features of the considered transformations.

When analyzing the solution of system (1)–(7), it is convenient to use the integral degrees of decomposition and ordering $0 < S_{dec} < 1$ and $0 < S_\eta < 1$

$$S_{dec} = \frac{1}{2c_0(1-c_0)L^n}\int|c(\mathbf{r}) - c_0|\,d\mathbf{r},$$
$$S_\eta = \frac{2}{L^n}\int|\eta(\mathbf{r})|\,d\mathbf{r}, \tag{8}$$

where n is the task dimension, and c_0 is the specimen-average concentration of a selected component. The numerical solution of Eqs. (4)–(7) was performed using the dimensionless coordinates x/L, the time $\tau = (D_{def}/L^2)\,t$, and the velocity of a defect $v_{def} = V_{def}L/D_{def}$.

The proposed model is similar to the regular solid solution model [46], but differs from it by taking into account the ordering (the case of $\theta \neq 0$) and the local change in the energy parameters on structural defects (Eqs. (2)–(3)). In contrast to the model of the diffusion cutting of precipitates [23, 25] and the known models of segregations on moving GBs [39, 41, 42], this model takes into account the change on a defect not only for the impurity dissolution energy $\varepsilon(\mathbf{r})$, but also for the mixing and ordering energies $\nu(\mathbf{r})$ and $\theta(\mathbf{r})$ and does not concretizes the driving force for the migration of defects. The parametrization of this model is discussed in Appendix.

3. SEGREGATIONS ON MOVING GRAIN BOUNDARIES

The formation of segregations is governed by the change in the energy of an impurity atom upon its displacement from the volume onto the boundary of a grain (i.e., by the segregation energy) $\delta\varepsilon(r)$ [39, 48]. Under SPD, segregations may appear at a rather low temperature (~300 K) in the broad near-boundary layer (see the discussion in [26, 49]). In the work [13], it has been hypothesized that the kinetics of the formation of such segregations is controlled not by bulk diffusion, but by the processes occurring at the boundary of a grain. A moving GB captures and carries the impurity atoms, so the segregation formation rate is multiply increased.

To demonstrate the qualitative features of interaction between moving defects and impurities, let us consider a one-dimensional model and confine our consideration to the case of an ideal solid solutions ($\nu = 0, \theta = 0$) [46]. At first, let us consider the situation when a defect moves at a constant velocity V_{def}.

The evolution of the maximum impurity concentration on a grain boundary during its motion is illustrated in Fig. 1a. Segregation on a motionless GB ($v_{GB} = 0$) is controlled by bulk diffusion ($D_b \ll D_{GB}$) and, for this reason, does not have enough time to appear on the considered time scale (curve *1*). On the contrary, a moving GB entrains impurity atoms such that the formation of a segregation is generally governed by the velocity of its motion (curves *2–4*). If a grain boundary moves at a low velocity, impurity atoms can follow it. If the velocity of a grain boundary is above a critical level, the diffusion in the direction perpendicular to the boundary has no enough time to provide the redistribution of atoms, and the concentration on the grain boundary decreases (curve *4*). Setting the characteristic diffusion time $t = d^2/D_{GB}$, for which an atom crosses the boundary, equal to the time $t = d/V_{GB}$, for which the grain boundary displaces at a distance equal to its width, we find the estimate for the

optimal GB velocity, which provides the most efficient development of segregations,

$$V_{GB}^{(opt)} = D_{GB}/d. \quad (9)$$

The effect of the entrainment of segregations by a moving GB is illustrated in Fig. 1b, which demonstrates the dependence of the impurity concentration attained on a grain boundary by a certain time moment, on the GB velocity (curves *1* and *2*).

It can be seen that the maximum value of c_{GB} grows with time and displaces towards lower velocities. Hence, the maximally possible segregation can be expected in this model on a motionless GB, but at an infinitely great exposure time, being in agreement with the results [37].

According to the existing notions [50], the motion of a boundary is implemented via the migration of steps, which is controlled by the self-diffusion of matrix atoms or implemented in an athermal fashion due to the effect of grain boundary sliding mechanisms [51]. The existence of segregations on a grain boundary will lead to its hindering due to the interaction of impurity atoms with steps, so the velocity of a grain boundary ceases to be an independent parameter. Let us take into account the impurity hindering of a grain boundary and write the migration velocity as

$$\tilde{v}_{GB}(t) = v_{GB}(1 - K(c_{max}(t) - c_0)), \quad (10)$$

where v_{GB} and $\tilde{v}_{GB}(t)$ are the initial and current velocities of a grain boundary, respectively, $c_{max}(t)$ is the maximum concentration attained on a grain boundary, c_0 is the average (initial) concentration of an impurity in a specimen, and K is the parameter characterizing the efficiency of hindering on impurity.

Curve *3*' in Fig. 1a and curves *1*' and *2*' in Fig. 1b (describing the dependence of the concentration on a grain boundary on its velocity v_{GB}) show that the hindering of a grain boundary stabilizes the intermediate segregation formation stages near the critical value $c_{max}^{cr} = c_0 + 1/K$, at which the "trapping" of a grain boundary takes place (velocity $\tilde{v}_{GB}(t) \equiv 0$). A further increase in the concentration on a grain boundary is a slow process controlled by the bulk diffusion coefficient D_b. The attainment of saturation by curves *1*' and *2*' in Fig. 1b argues for the fact that a grain boundary stops when segregation reaches c_{max}^{cr} within a broad range of initial GB velocities v_{GB}.

It should be noted that the maximum concentration value attained on a grain boundary (Fig. 1) was obtained regardless of the interaction between impurity atoms. At a positive mixing energy ($\nu > 0$), the repulsion between impurity atoms will reduce the formation of segregations (see the discussion in [26]), while the formation of precipitates on a grain boundary should be expected at $\nu < 0$.

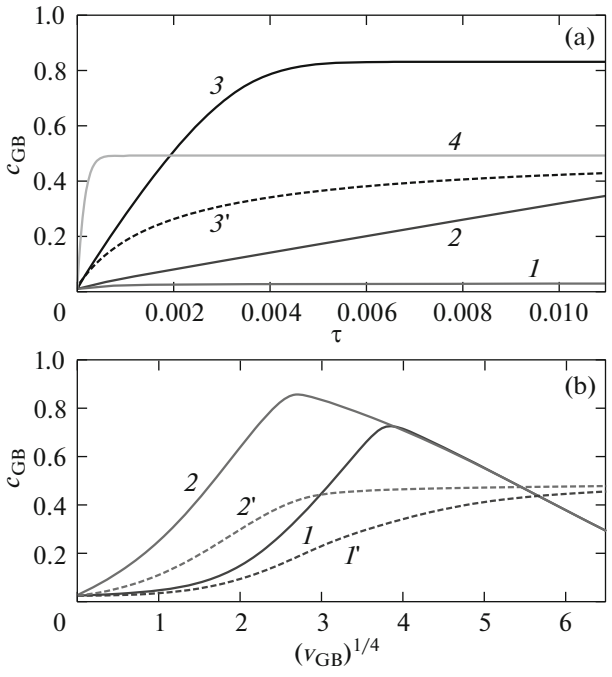

Fig. 1. (a) Impurity concentration evolution on a grain boundary at its velocity v_{GB} of (*1*) 0, (*2*) 12.5, (*3*) 100, and (*4*) 800; curve *3*' corresponds to (*3*) with consideration for the hindering of a grain boundary at $K = 2$; (b) impurity concentration attained on a grain boundary by the time moment τ of (*1*, *1*') 0.002 and (*2*, *2*') 0.02 versus initial velocity of a grain boundary in (*1*, *2*) without and (*1*', *2*') with the hindering of a grain boundary by impurity atoms. Average impurity concentration $c_0 = 0.01$, segregation energy $\delta\varepsilon = -0.3$ eV/atom, $T = 500$ K, $D_{GB}/D_b = 10^5$, $d/L = 0.005$.

A similar consideration can be performed not only for segregations on a grain boundary, but also for the formation of impurity atmospheres on moving dislocations. However, the sliding of dislocations is implemented for the times, which are much shorter than the characteristic diffusion times. For this reason, the appearance of the considered defects may be expected only for relatively slow dislocation migration mechanisms (climb, thermally activated motion of dislocations in ordered alloys).

4. DISORDERING OF ALLOY AND FORMATION OF NONEQUILIBRIUM PHASES

The change in the ordering energy $\theta(\mathbf{r})$ near a defect (dislocation or grain boundary) leads to the local shift of the ordering temperature. Actually, Eqs. (1) and (7) give the Bragg–Williams condition for a locally equilibrium state ($dF/d\eta = 0$) [44]

$$-\frac{4\theta(\mathbf{r})\eta(\mathbf{r})}{kT} = \ln\left[\frac{(c(\mathbf{r}) + \eta(\mathbf{r}))(1 - c(\mathbf{r}) + \eta(\mathbf{r}))}{(c(\mathbf{r}) - \eta(\mathbf{r}))(1 - c(\mathbf{r}) - \eta(\mathbf{r}))}\right]. \quad (11)$$

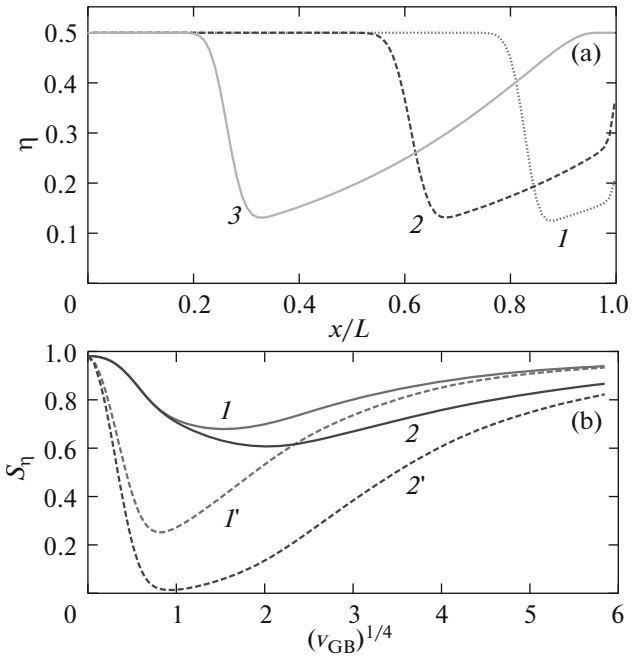

Fig. 2. (a) Profiles of the order parameter η at time moments τ of (*1*) 0.02, (*2*) 0.04, and (*3*) 0.07 for the displacement of a grain boundary from the initial position $x/L = 1$ to the position $x/L = 0$ at a velocity $v_{GB} = 10$ at $D_{GB}/D_b = 10^2$; (b) specimen-average degree of ordering versus defect velocity after (*1*, *1*') one and (*2*, *2*') five passages at D_{GB}/D_b of (*1*, *2*) 10^2 and (*1*', *2*') 10^5; $c_0 = 0.5$, $\kappa_0 L^2 = 250$, $\nu = \delta\varepsilon = 0$, $\theta_b = -0.3$ eV, $\delta\theta = +0.3$ eV, $T = 500$ K, $d/L = 0.03$.

The starting ordering temperature follows from Eq. (11) in the limit $\eta(\mathbf{r}) \to 0$, i.e.,

$$kT_{ord}(\mathbf{r}) = -2\theta(\mathbf{r})c(\mathbf{r})(1 - c(\mathbf{r})). \quad (12)$$

Taking into account the fact that the initial ordered state corresponds to a minimum alloy free energy (1), it is natural to expect that the free energy of an ordered state in a distorted lattice near a defect grows, i.e., $\delta\theta > 0$. As a result, according to Eq. (12), the ordering temperature on a defect should be expected to decrease, i.e.,

$$T_{ord} \to T_{ord}^{def} = T_{ord} - 2\delta\theta c(1 - c)/k,$$

and local disordering will be observed in an alloy within the temperature range $T_{ord}^{def} < T < T_{ord}$. The disordered state is frozen after the displacement of a defect due to the difference between the diffusion coefficients D_{def} and D_b.

The results of calculations for the local ordering parameter η at different time moments during the passage of grain boundary through the grain are shown in Fig. 2a. It can be seen that an extensive partially disordered region is left behind the moving GB. The degree of disordering is determined by the velocity of this GB and the rate of relaxation processes, i.e., by the ratio D_{GB}/D_b. As can be seen from Fig. 2b, there exists a certain velocity value v_{GB}^{opt} (which is much lower than the sound velocity, see Appendix), at which the greatest disordering is attained; atomic order is restored behind a grain boundary at $v_{GB} < v_{GB}^{opt}$, but disordering has not enough time to appear at $v_{GB} > v_{GB}^{opt}$. Disordering in the alloy is continued in the case of repeated passages of a grain boundary through a grain (which were implemented in the process of modeling with the use of periodic boundary conditions) (see curves *1* and *2*, *1*' and *2*'). For this reason, complete disordering may be expected at a high ratio D_{GB}/D_b under prolonged treatment even at a low concentration of defects.

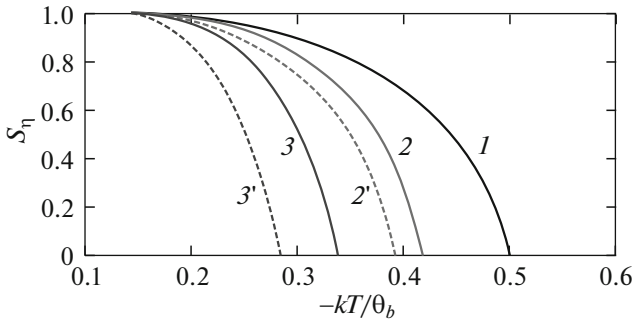

Fig. 3. Specimen-average degree of ordering versus temperature (*1*) in the absence of defects and (*2*, *2*'), (*3*, *3*') in a steady regime for the multiple passage through a GB specimen at a velocity $v_{def} = 10$, $\delta\theta/|\theta_b|$ of (*2*, *2*') 0.25 and (*3*, *3*') 0.5, D_{def}/D_b of (*2*, *3*) 10^2 and (*2*', *3*') 10^5, and other parameters the same as for Fig. 2.

Figure 3 demonstrates the temperature dependence of the specimen-average degree of ordering in the absence of a grain boundary (curve *1*) and in the steady-state regime attained after the repeated passages of a grain boundary through the considered volume (curves *2*, *2*' and *3*, *3*'). It can be seen that the higher is the ratio D_{def}/D_b or $\delta\theta/|\theta_b|$, the greater is a decrease in the starting ordering temperature T_{ord}^{def}.

We have assumed above that only the ordering energy changes on a defect ($\delta\theta \neq 0$, $\delta\varepsilon = 0$). If $\delta\varepsilon \neq 0$, the development of segregations for one of the alloy components may stimulate its disordering even at $\delta\theta = 0$. When a defect is displaced, it makes a segregation that follows it, while the attained disordered state may prove to be frozen (see Fig. 4). On the other hand, disordering in the case of hindering a defect by segregations ($K \neq 0$, see Eq. (10)) is possible, if the initial velocity of a defect is higher than the critical value; otherwise, segregations stop a defect and, correspondingly, no disordering is implemented.

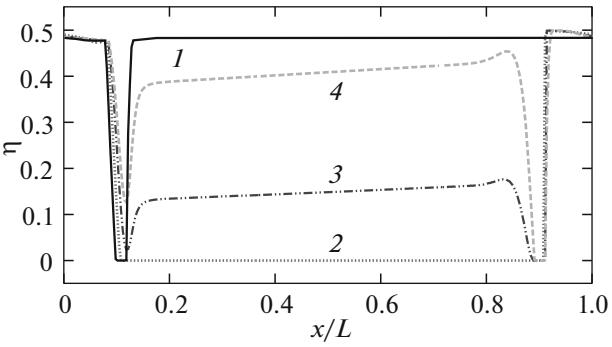

Fig. 4. Attained profiles of the order parameter η after the displacement of a grain boundary from the position $x/L = 0.9$ to the position $x/L = 0.1$ at a velocity v_{GB} of (*1*) 1, (*2*) 5, (*3*) 15, and (*4*) 25; $c_0 = 0.5$, $D_{GB}/D_b = 10^3$, $\kappa_0 L^2 = 500$, $\nu = 0$, $\delta\varepsilon = -0.35$ eV, $\theta_b = -0.3$ eV, $T = 500$ K, $d/L = 0.05$.

In the general case, an ordered state in equilibrium is provided by the requirement $\theta < \nu$ (see Eq. (1)); i.e., the tendency to possible decomposition is suppressed in virtue of ordering. However, local disordering may occur in the area of a defect as a result of either the change in the energy θ or the segregation of one of the components. Then the development of spinodal decomposition can take place after disordering on the defect.

The kinetics of decomposition in an ordered phase, when the energy θ changes at a grain boundary (which displaces from the position $y/L = 0.9$ to the position $y/L = 0.5$ and stops), is illustrated in Fig. 5. Spinodal decomposition develops on the boundary during its motion (Fig. 5, upper row), and the system relaxes to an equilibrium ordered state under further exposure at a rate characterized by the bulk diffusion coefficient D_b (Fig. 5, lower row).

5. DISSOLUTION OF PRECIPITATES AND FORMATION OF DISSIPATIVE STRUCTURES

In the absence of ordering ($\theta = 0$) at $\nu < 0$, Eq. (4) describes the decomposition with the formation of a two-phase state, and the equilibrium limits of solubility in phases are characterized by the binodal of a regular solid solution [46]

$$\frac{\nu}{kT} = \frac{1}{1-2c}\ln\left(\frac{c}{1-c}\right). \qquad (13)$$

Let us confine our consideration to the situation, when the mixing energy ν is the same everywhere, while the dissolution energy $\varepsilon(\mathbf{r})$ and the diffusion coefficient are locally changed on a defect (dislocation or grain boundary) to provide segregations of one of the components. If a defect is motionless, segregations stimulate the appearance of precipitates of equilibrium phases, thus increasing the degree of decomposition.

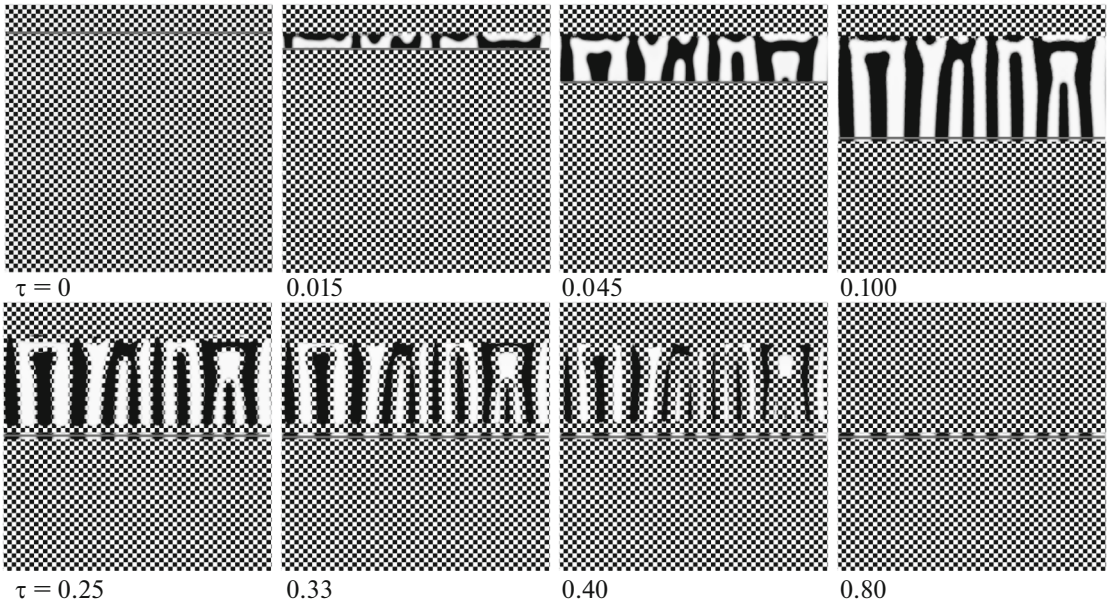

Fig. 5. Decomposition of an equilibrium ordered phase due to the change in the ordering energy on a grain boundary (its position is marked with a horizontal line) displacing from the position $y/L = 0.9$ to the position $y/L = 0.5$ and restoration of the ordered state in the course of exposure; $\theta = -0.3$ eV, $\delta\theta = +0.3$ eV, $D_{GB}/D_b = 10^2$, $v_{GB} = 4$, $c_0 = 0.5$, $\kappa_0 L^2 = 250$, $\nu = -0.14$ eV, $\delta\varepsilon = 0$, $T = 500$ K, $d/L = 0.03$, $R/L = 0.0016$. Depleted and enriched phases appearing in the process of decomposition are shown in white and black colors, respectively, and the other part of this figure corresponds to the initial ordered phase.

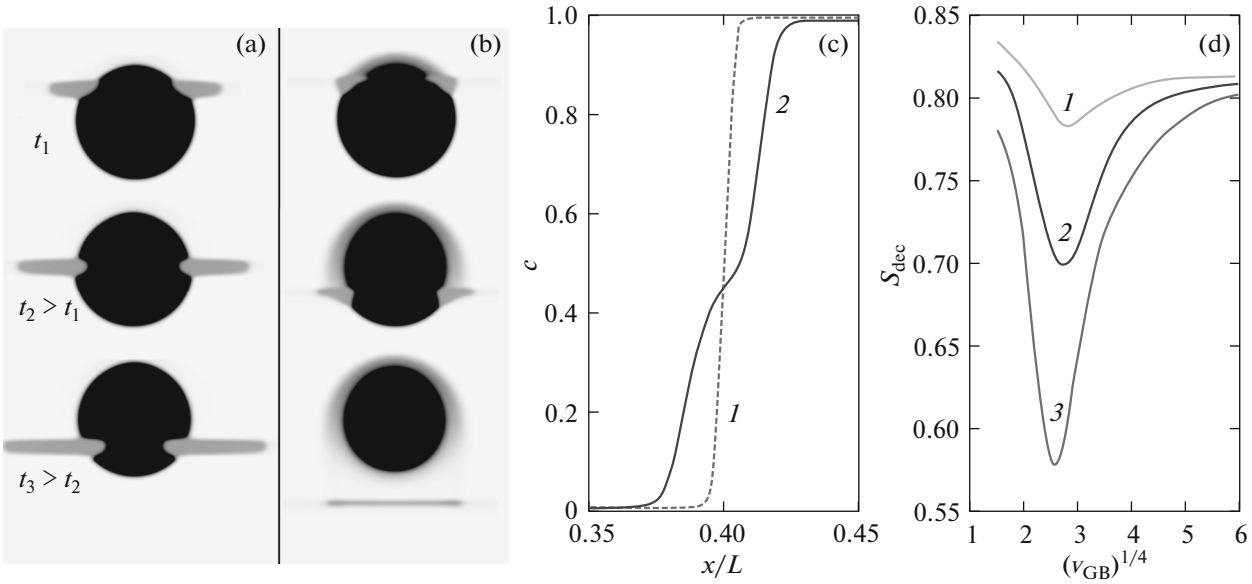

Fig. 6. Distribution of alloy component in the neighborhood of a precipitate at different times in the case of one passage of a grain boundary at a velocity v_{GB} of (a) 10 and (b) 60; (c) concentration profiles (*1*) on the interface of an initial precipitate and (*2*) after the passage of a grain boundary at $v_{GB} = 60$; (d) degree of decomposition versus velocity of a grain boundary after (*1*) one, (*2*) five, and (*3*) fifteen passages. $D_{GB}/D_b = 10^5$, $\delta\varepsilon^{(m)} = -0.15$, $\delta\varepsilon^{(p)} = 0.10$, $\nu = -0.3$ eV/atom, $T = 700$ K, $d/L = 0.03$, $R/L = 0.1$.

However, if a defect moves and crosses the volume of precipitates, the different scenario with the dissolution of precipitates can be implemented.

Let the energy of segregation on a defect $\delta\varepsilon$ be different in the neighboring phases, thus stimulating the redistribution of alloy components along a defect between the matrix and the volume of a precipitate. If the energy of segregation in the matrix is higher (by its absolute value) than in a precipitate, the flow of atoms along a grain boundary (or a dislocation tube) from the volume of a precipitate into the matrix occurs, thus promoting the dissolution of this precipitate. The thermodynamic stimulus of decomposition is determined by the mixing energy ν and acts as a competing factor.

Let us confine our consideration to the simple model and classify the areas with $c(\mathbf{r}) > 0.5$ as precipitates. Then it is possible to write for the energy of impurity segregation on a defect that

$$\delta\varepsilon(\mathbf{r}) = \delta\varepsilon^{(m)} + h[c(\mathbf{r}) - 0.5](\delta\varepsilon^{(p)} - \delta\varepsilon^{(m)}), \qquad (14)$$

where $\delta\varepsilon^{(p)}$ and $\delta\varepsilon^{(m)}$ are the energies of segregation in the areas of a boundary inside and outside the volume of a precipitate, respectively, and $h(c)$ is the smoothened Heaviside function (see Appendix).

The substitution of Eq. (14) into Eq. (1) leads to the result, which can be interpreted as a local change in the mixing energy ν by the value $\delta\varepsilon^{(pm)} = \delta\varepsilon^{(p)} - \delta\varepsilon^{(m)}$. Then it follows from Eq. (13) that the starting temperature of decomposition in a homogeneous alloy decreases on a defect

$$kT_{dec}^{def} = (\nu + \delta\varepsilon^{(pm)})\frac{1 - 2c_0}{\ln[c_0/(1 - c_0)]}, \qquad (15)$$

and the local dissolution of a precipitate is possible at a rather high value of $\delta\varepsilon^{(pm)}$.

The results of modeling the passage of a grain boundary through an equilibrium phase precipitate are shown in Figs. 6a and 6b. It can be seen that a segregation with an intermediate composition ($c \sim 0.5$) is formed at small v_{GB} and completely entrained by a defect, and the form of this precipitate remains similar to the initial one. At a high velocity of a grain boundary, when $V_{GB} > D_{GB}/d$ (see Eq. (9)), the segregation has not enough time to follow the grain boundary and, as a result, the interface of the precipitate behind the grain boundary becomes abnormally broadened (Fig. 6b) and "frozen" in a nonequilibrium state due to a low bulk diffusion rate. The concentration profiles on the initial (equilibrium) interface and after the passage of the grain boundary are shown in Fig. 6c. Hence, the degree of dissolution for a precipitate after a single passage of a grain boundary is determined by the segregation capacity of a grain boundary at low v_{GB} and by the surface area of a precipitate at high v_{GB}.

Figure 6d demonstrates the dependences of the specimen-average degree of decomposition S_{dec} on the velocity of a grain boundary after one (curve *1*), five (curve *2*), and fifteen (curve *3*) passages. It can be seen

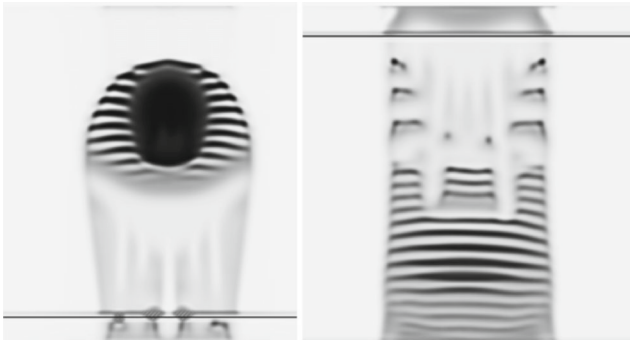

Fig. 7. Kinetics of the formation of a modulated structure in case of the multiple passage of a defect through a precipitate at $v_{\text{def}} = 80$, $D_{\text{def}}/D_b = 10^2$, $\delta\varepsilon^{(m)} = -0.15$, $\delta\varepsilon^{(p)} = +0.15$, $\nu = -0.3$ eV/atom, $T = 700$ K, and $d/L = 0.03$.

that there exists an optimal velocity, which provides maximal alloy homogenization (for a specified number of passages).

The result of the multiple passage of defects through a precipitate depends on the ratio between the energies $\delta\varepsilon^{(pm)}$ and ν, the diffusion coefficients D_{def} and D_b, the average concentration c_0, and the velocity of defects. A variety of possible regimes is confined to the three main scenarios: (1) a precipitation is preserved as a whole, but its size is changed (the case of a small change in $\delta\varepsilon^{(pm)}$), (2) a precipitate is completely dissolved (the case of low temperatures and high $\delta\varepsilon^{(pm)}$), and (3) there appears a dispersed state (or a pattern), which remains relatively stable in the course of further treatment (the case of moderate temperatures).

The typical pictures of the formation of a modulated structure during the dissolution of a solitary precipitate are shown in Fig. 7. A specific feature of this regime is a relatively high bulk diffusion rate ($D_{\text{def}}/D_b = 100$), which results in the competition between the processes controlled by diffusion on defects and bulk diffusion responsible for the return back to the two-phase equilibrium. For this reason, the spinodal decomposition processes, whose rate is controlled by bulk diffusion, are developed in the neighborhood of a precipitate after the passage of a defect. The passage of the next defect through the precipitate leads to the broadening of the area with a nonequilibrium composition. At great times of treatment, the initial precipitate is completely dissolved with the formation of a quasi-periodic distribution of concentrations; i.e., inversion of spinodal decomposition occurs.

6. DISCUSSION OF RESULTS

The objective of this work was to perform the analysis of qualitative features in the nonequilibrium diffusional transformations induced by moving defects under severe plastic deformation (SPD) in the region of moderate temperatures, when bulk diffusion is frozen. For this reason, we do not consider the mechanical mass transfer during the sliding of dislocations and confined our consideration to the simple model, which took into account the processes of abnormal diffusion on moving defects. We demonstrate that the local change of alloy parameters and accelerated diffusion on the defects may lead to a great variety of nonequilibrium phase transformations. The obtained results give us an opportunity to take a fresh look at the development of structural and phase transformations under SPD in the region of moderate temperatures.

In the proposed model, the type of defects (dislocation or grain boundary) has not been concretized in most cases. It is known that the dislocation mode of plastic deformation predominates in coarse-grain specimens [20], while low-temperature dynamic recrystallization accompanied by the migration of grain boundaries is implemented upon the transition to a nanocrystalline state [36]. The disordering and dissolution of small precipitates usually require no transition to a nanocrystalline state [4, 15] and, in principle, can be provided by the passage of dislocations. At the same time, the implementation of abnormal mechamical alloying in nanocrystalline specimens seems to require the migration of grain boundaries. Let us note that even one passage of a grain boundary through a specimen can lead to the profound consequences comparable with the result from the passage of many dislocations.

The known models for the formation of segregations on moving grain boundaries [39] do not pay sufficient attention to the fact that the kinetics of segregations at a low temperature is controlled by grain boundary diffusion. We have demonstrated that the motion of a grain boundary in this case may be critically important for the development of segregations. Herewith, there exists the optimal GB velocity, at which the development of segregations is most efficient.

The disordering of intermetallides under SPD was revealed for the first time in the Fe–Pt and Co–Pt systems and accompanied by amorphization in the Y–Co and Gd–Co systems [1]. This transformation is frequently fast and does not require intensive and prolonged treatment (see the reviews [2, 17]), thus indirectly evidencing for a low density of defects in the volume of a material. The widely spread explanation [17] of this phenomenon by immediate mixing during the sliding of partial dislocations through the volume of grains encounters the difficulty consisting in the fact that the penetration of dislocations into the volume of grains is suppressed at least in a nanocrystalline state (which frequently precedes disordering and amorphization) [20]. In addition, the disordering of an alloy can hardly be provided by the motion of superstructural dislocations, as they have a relatively small effect

on its thermodynamic parameters and do not destroy the chemical order after their passage. On the other hand, low-temperature dynamic recrystallization is called a necessary condition of transition to a nanocrystalline state [36], and this allows us to presume an important role of moving grain boundaries in the disordering of nanocrystalline alloys.

The dissolution of intermetallide and carbide precipitates under SPD was repeatedly observed in experiments (see, e.g., [4]), and this phenomenon is usually explained engaging the notions about mechanical mixing in siding bands [15–17] or "diffusion cutting" [23–25] implemented at a rather great dimensional mismatch between the atoms of the matrix and a dissolved component (e.g., interstitial admixtures).

In the model proposed by us, the mechanical cutting of precipitates is considered, and it is taken into account that the change in the "chemical" energy of an impurity atom can make an essential contribution in addition to the elastic one. When a defect passes through a precipitate, the flows of atoms along the defect due to the difference between the energies of segregation in the precipitate and the matrix occurs, thus leading to the partial dissolution of the precipitate and the broadening of the phase interface (Fig. 6b). The latter feature is a characteristic sign for the action of such a mechanism. The multiple passages of defects enable the appreciable reduction of precipitates in size and even their complete dissolution. A similar scenario of microstructural evolution under SPD was observed in [4, 52, 53].

The change in the energy of chemical bonds on a defect may lead to that impurity atoms segregate on grain boundaries in one phase and, on the contrary, pushed off grain boundaries in the other phase; i.e., the parameter $\delta\varepsilon$ switches its sign in the precipitate as compared with matrix, as implemented in calculations (Figs. 6 and 7). Strictly speaking, such a correspondence between the segregation energies is not obligatory. To provide the dissolution of precipitates upon the passage of dislocations or grain boundaries through them, it is sufficient for the energy of an impurity atom to decrease upon its displacement from a precipitate into the matrix along a defect. A similar situation seems to take place upon the passage of dislocations through cementite particles, where the appreciable depletion of cementite in carbon takes place [53].

Some examples for the decomposition of alloys with the formation of nonequilibrium phases under SPD are discussed in [1, 5–7, 54–57]. Thus, in particular, the disordering and amorphization of the initial phase occurred in the alloy $Nd_2Fe_{14}B$ together with the precipitation of α-Fe nanocrystals [5, 6] (contrary to the equilibrium phase diagram). The opinions that the implementation of nonequilibrium transformation in this system is associated with the change in the thermodynamic properties of the alloy due to the accumulated energy of defects were formulated in [56]. In the developed approach, which considers moving defects, the assumption about their accumulation in a material is not obligatory. It should be noted that the diffusion processes are likely to be implemented in these experiments only in a local fashion in the area of a shear band; otherwise, bulk diffusion would promote the restoration of atomic order and the relaxation of an amorphous state.

The formation of steady dispersed states (patterns) in alloys AgCu [8] and FeCr [9] was also observed under SPD at moderate temperatures due to the competition between bulk diffusion (which provides decomposition in compliance with the equilibrium phase diagram) and the development of a nonequilibrium transformation (mechanical alloying) under treatment. It seems that these states may be considered as an example of dissipative structures [58], which appear in open systems far from thermodynamic equilibrium. According to the notions [8, 17], mechanical alloying is provided by the reduction of precipitates in size and the immediate mixing of atoms due to the sliding of dislocations in mutually crossing planes. However, according to [3], mechanical alloying is accelerated upon the transition to a nanocrystalline state, when the penetration of dislocations into the volume of grains is complicated [20], and this seems to evidence for an important role played by the migration of grain boundaries in this case. Our model reveals a new mechanism of mechanical alloying and the formation of dissipative structures, related to the diffusion on moving defects (dislocations and grain boundaries) at moderate temperatures, when this diffusion is not negligibly small.

The discussed results were obtained within the framework of a simple model, which does not take into account many details in the interaction of impurity atoms with dislocations or grain boundaries, under the assumption about a constant velocity of defects. Nevertheless, it is possible to presume that our conclusions correctly reflect the qualitative features of change in the phase and structural state of alloys under SPD.

7. CONCLUSIONS

The model describing the effect of moving defects (dislocations, grain boundaries) on the development of nonequilibrium phase transformations under severe plastic deformation has been formulated. It has been demonstrated that the disordering of an alloy, the appearance of nonequilibrium phases, and the formation of supersaturated solid solutions and dissipative structures can be implemented due to the local change in the thermodynamic properties of this alloy and the accelerated diffusion on moving defects. It has been shown that an optimal defect velocity exists, at which the mentioned transformations are most efficiently implemented, in the case of one passage of a defect, and the accumulative effect takes place in the case of

multiple passages. The obtained results provides the possibility to give a qualitative explanation for the specific features of change in the phase and structural state of alloys under severe plastic deformation at moderate temperatures, when the diffusion on defects is not negligibly small.

APPENDIX

MODEL PARAMETRIZATION

In the presented calculation, the size of a grain is characterized by the ratio L/d and attains 30–200 nm (the characteristic width of a defect d was taken equal to 1 nm). The disturbance shape function near a defect was taken in the form

$$\Omega(\mathbf{r}-\mathbf{r}_{\text{def}}) = \left(1+\left[\frac{2}{d}(\mathbf{r}-\mathbf{r}_{\text{def}})\right]^{12}\right)^{-1}. \quad \text{(A.1)}$$

In the case of switching in the energy of dissolution in the phases depending on the concentration (see Eq. (14)), we used the smoothened Heaviside function

$$h = \left(1+\exp\left(-\frac{c(\mathbf{r})-0.5}{0.02}\right)\right)^{-1}. \quad \text{(A.2)}$$

The temperature was selected from the range of 500–700 K, at which the typical values of D_{GB} are 10^{-13}–10^{-19} m^2/s [59]. As follows from the formula $v_{\text{def}} = V_{\text{def}}L/D_{\text{def}}$, the range considered in the calculations for the velocities of defects V_{def} is 10^{-5}–10^{-14} m/s, and the characteristic time of processes are estimated by the formula $\tau = D_{\text{def}}/L^2t$ with a spread of values of 10^{-4}–10^5 s. In experiments, the abnormal transformations under SPD are usually completed for several seconds and, in principle, agree with this estimate. It is also worth noting that the generation of nonequilibrium vacancies under SPD [60] may increase the diffusion coefficient D_{def} (and, correspondingly, the characteristic rates of processes) by 10 orders of magnitude. Moreover, the grain boundary diffusion coefficient on nonequilibrium grain boundaries formed under SPD may grow by 3–5 orders of magnitude in comparison with ordinary conditions as a result of distortion in the lattice within the broad near-boundary area [61].

The rate of ordering processes in the theoretical models [44, 45] is determined by the time of a single atomic jump, which is much shorter than the characteristic diffusion times, whence it follows that $\kappa_0 L^2 \gg 1$. In experiments, the incubation period of ordering was observed [11, 62], probably due to the need for the implementation of long-range ordering and, in certain cases, crystal lattice rearrangement decelerating the development of this transformation.

ACKNOWLEDGMENTS

This work was performed within the state task on the subjects "Magnet" (project no. N AAAA-A18-118020290129-5) and "Structure" (project no. N AAAA-A18-118020190116-6).

REFERENCES

1. A. E. Ermakov, Fiz. Met. Metalloved., No. 11, 4 (1991).
2. H. Bakker, P. I. Loeff, and A. W. Weeber, Def. Dif. Forum **66–69**, 1169 (1989).
3. C. Suryanarayana, Prog. Mater. Sci. **46**, 1 (2001).
4. V. V. Sagaradze and V. A. Shabashov, Phys. Met. Metallogr. **112**, 146 (2011).
5. A. G. Popov, V. S. Gaviko, and N. N. Shchegoleva, L. A. Shreder, V. V. Stolyarov, D. V. Gunderov, X. Y. Zhang, W. Li, and L. L. Li, Phys. Met. Metallogr. **104**, 238 (2007).
6. A. G. Popov, V. S. Gaviko, A. S. Ermolenko, N. N. Shchegoleva, V. V. Stolyarov, and D. V. Gunderov, in *Structure and Properties of Nanocrystalline Materials, Collection of Articles* (Yekaterinburg, 1999) [in Russian].
7. V. A. Tsurin, V. A. Barinov, and S. B. Pupyshev, Tech. Phys. Lett. **21**, 449 (1995).
8. F. Wu, D. Isheim, P. Bellon, and D. N. Seidman, Acta Mater. **54**, 2605 (2006).
9. G. le Caër, S. Begin-Colin, and P. Delcroix, in *Materials Research in Atomic Scale by Mössbauer Spectroscopy*, Ed. by M. Mashlan, M. Miglierini, and P. Schaaf (Springer, Dordrecht, 2003), p. 11.
10. B. B. Straumal, S. G. Protasova, A. A. Mazilkin, E. Rabkin, D. Goll, G. Schutz, B. Baretzky, and R. Z. Valiev, J. Mater. Sci. **47**, 360 (2012).
11. O. S. Novikova and A. Yu. Volkov, Phys. Met. Metallogr. **114**, 162 (2013).
12. M. Herbig, D. Raabe, Y. J. Li, P. Choi, S. Zaefferer, and S. Goto, Phys. Rev. Lett. **112**, 126103 (2014).
13. B. B. Straumal, B. Baretzky, A. A. Mazilkin, F. Philipp, O. A. Kogtenkova, M. N. Volkov, and R. Z. Valiev, Acta Mater. **52**, 4469 (2004).
14. X. Sauvage, A. Ganeev, Y. Ivanisenko, N. Enikeev, M. Murashkin, and R. Valiev, Adv. Eng. Mater. **14**, 968 (2012).
15. H. Bakker, G. F. Zhou, and H. Yang, Prog. Mater. Sci. **39**, 159 (1995).
16. P. Bellon and R. Averback, Phys. Rev. Lett. **74**, 1819 (1995).
17. G. Martin and P. Bellon, Solid State Phys. **50**, 189 (1997).
18. G. A. Dorofeev and E. P. Elsukov, Phys. Met. Metallogr. **103**, 593 (2007).
19. E. P. Yelsukov, G. A. Dorofeev, V. A. Barinov, T. F. Grigor'eva, and V. V. Boldyrev, Mater. Sci. Forum **269–272**, 151 (1998).
20. V. V. Rybin, *Large Plastic Deformations and Fracture of Metals* (Metallurgiya, Moscow, 1986) [in Russian].
21. J. Eckert, J. Holzer, C. Krill, and W. Johnson, J. Appl. Phys. **73**, 2794 (1993).

22. M. A. Shtremel', Metal Sci. Heat Treatment **8**, 10 (2002).
23. H. Gleiter, Acta Meter. **16**, 455 (1968).
24. B. Ya. Lyubov and V. A. Shmakov, Fiz. Met. Metalloved. **29**, 968 (1970).
25. B. Ya. Lyubov, *Diffusion Processes in Non-Homogeneous Solid Media* (Nauka, Moscow, 1981) [in Russian].
26. L. E. Karkina, I. N. Karkin, A. R. Kuznetsov, I. K. Razumov, P. A. Korzhavyi, and Yu. N. Gornostyrev, Comput. Mater. Sci. **112**, 18 (2016).
27. A. Y. Lozovoi, A. T. Paxton, and M. W. Finnis, Phys. Rev. B **74**, 155416 (2006).
28. R. W. K. Honeycombe, *Plastic Deformation of Metals* (Hodder Arnold, London, 1984).
29. B. Q. Li and F. E. Wanter, Acta Mater. **46**, 5483 (1998).
30. A. R. Yavari, P. J. Desré, and T. Benameur, Phys. Rev. Lett. **68**, 2235 (1992).
31. I. K. Razumov, Russ. J. Phys. Chem. A **84**, 1485 (2010).
32. R. D. Doherty, Met. Sci. **16**, 1 (1982).
33. H. Octor and S. Naka, Philos. Mag. Lett. **59**, 229 (1989).
34. S. Naka, H. Octor, E. Bouchaud, and T. Khan, Scripta Met. **23**, 501 (1989).
35. E. Bouchaud, S. Naka, and H. Octor, Colloq. Phys. **51**, 451 (1990).
36. A. M. Glezer and M. S. Metlov, Phys. Solid State **52**, 1162 (2010).
37. J. W. Cahn, Acta Met. **10**, 789 (1962).
38. K. Lücke and H. P. Stüwe, Acta Met. **19**, 1087 (1971).
39. P. Lejček, Springer Ser. Mater. Sci. **136**, 1 (Springer, Berlin, 2010).
40. G. Gottstein and L. S. Shvindlerman, *Grain Boundary Migration in Metals: Thermodynamics, Kinetics, Applications* (CRC, Boca Raton, 1999).
41. P. R. Cha, S. G. Kim, D. H. Yeon, and J. K. Yoon, Acta Mater. **50**, 3817 (2002).
42. J. Li, J. Wang, and G. Yang, Acta Mater. **57**, 2108 (2009).
43. A. G. Khachaturyan, *The Theory of Phase Transitions and Structure of Solid Solutions* (Nauka, Moscow, 1974) [in Russian].
44. J.-F. Gouyet, M. Plapp, W. Dieterich, and P. Maas, Adv. Phys. **52**, 523 (2003).
45. I. K. Razumov, Yu. N. Gornostyrev, and A. Ye. Yermakov, Rev. Adv. Mater. Sci. **18**, 767 (2008).
46. J. Christian, *Theory of Transformations in Metals and Alloys* (Pergamon, Oxford, 1975; Mir, Moscow, 1978).
47. S. M. Allen and J. W. Cahn, J. Phys. **38**, 7 (1977).
48. D. McLean, *Grain Boundaries in Metals* (Clarendon, Oxford, 1957; Metallurgizdat, Moscow, 1960).
49. I. K. Razumov, Russ. J. Phys. Chem. A **88**, 494 (2014).
50. G. Gottstein, D. A. Molodov, and L. S. Shvindlerman, Interface Sci. **6**, 7 (1998).
51. D. S. Gianola, S. van Petegem, M. Legros, S. Brandstetter, H. van Swygenhoven, and K. J. Hemker, Acta Mater. **54**, 2253 (2006).
52. V. T. Rakin and N. N. Buinov, Fiz. Met. Metalloved. **11**, 59 (1961).
53. Yu. Ivanisenko, W. Lojkowski, R. Z. Valiev, and H.-J. Fecht, Acta Mater. **51**, 5555 (2003).
54. V. A. Barinov, G. A. Dorofeev, L. V. Ovechkin, E. P. Elsukov, and A. E. Ermakov, Phys. Status Solidi A **123**, 527 (1991).
55. A. Ye. Yermakov, Mater. Sci. Forum **179–181**, 455 (1995).
56. E. I. Teitel', L. S. Metlov, D. V. Gunderov, and A. V. Korznikov, Phys. Met. Metallogr. **113**, 1162 (2012).
57. I. K. Razumov, Yu. N. Gornostyrev, and A. Ye. Yermakov, Phys. Met. Metallogr. **119** (12), 1133 (2018).
58. I. Prigogine, *Introduction to Thermodynamics of Irreversible Processes* (Wiley, Chichester, 1968).
59. *Diffusion in Solids Metals and Alloys*, Landolt-Börnstein New Series (Springer, Berlin, 1990), Vol. III/26.
60. T. Ungar, E. Schafler, P. Hanak, S. Bernstorff, and M. Zehetbauer, Mater. Sci. Eng. A **462**, 398 (2007).
61. V. V. Popov and A. V. Sergeev, Phys. Met. Metallogr. **118**, 1091 (2017).
62. B. Gwalani, T. Alam, C. Miller, T. Rojhirunsakool, Y. S. Kim, S. S. Kim, M. J. Kaufman, Yang Ren, and R. Banerjee, Acta Mater. **115**, 372 (2016).

Translated by E. Glushachenkova